Paper presented at the 10th International Conf.
on Hyperfine Interactions, Leuven, Aug. 28–Sept. 1

TRI–PP–95–48
August 1995

MUONIUM QUANTUM DIFFUSION AND LOCALIZATION IN CRYOCRYSTALS

V. STORCHAK
Kurchatov Institute, Kurchatov Sq. 1, Moscow 123182, Russia

J.H. BREWER and G.D. MORRIS
Canadian Institute for Advanced Research and Department of Physics, University of British Columbia, Vancouver, B.C., Canada V6T 2A3

We review our recent study of atomic muonium (μ^+e^- or Mu, a light isotope of the hydrogen atom) diffusion in the simplest solids — Van der Waals cryocrystals. We give experimental evidence of the quantum-mechanical nature of the Mu diffusion in these solids. The results are compared with the current theories of quantum diffusion in insulators. The predicted $T^{\pm 7}$ power-law temperature dependence of the Mu hop rate is observed directly for the first time in solid nitrogen (s-N_2) and is taken as confirmation of a two-phonon scattering mechanism. In solid xenon and krypton, by contrast, the one-phonon interaction is dominant in the whole temperature range under investigation due to the extremely low values of the Debye temperatures in those solids. Particular attention is devoted to processes of inhomogeneous quantum diffusion and Mu localization. It is shown that at low temperatures static crystal disorder results in an inhomogeneity of the Mu quantum diffusion which turns out to be inconsistent with diffusion models using a single correlation time τ_c. Conventional trapping mechanisms are shown to be ineffective at low temperatures in insulators. Muonium localization effects are studied in detail in solid Kr. In *all* the cryocrystals studied, muonium atoms turn out to be *localized* at the lowest temperatures.

1. Introduction

Many phenomena in solids at low temperatures are determined by tunneling motion of particles whose masses are large with respect to that of an electron. These phenomena take place in classical and quantum crystals, metals and insulators, semiconductors and superconductors, *etc.* The basic concept introduced in order to describe such effects is that of band motion (coherent tunneling) of a particle with a bandwidth Δ determined by the amplitude of particle's resonance transition [1,2]. Particle dynamics in a perfect crystal at $T = 0$ represents the simplest case of band motion.

At $T \neq 0$, however, tunneling occurs on a background of coupling with the excitations of the medium. Since Δ is small, this coupling is always

relatively strong. Therefore the tunneling kinetics in a solid is a problem of motion in a system with weak quantum correlations and a strong dynamic interaction with medium excitations [3]. The basic characteristic of the particle interactions with the medium excitations is the frequency Ω of phase correlation damping at neighboring equivalent positions of the particle. Even at low temperatures Ω can be as large as Δ; raising the temperature results in an exponential decrease of the coherent tunneling transition [3].

The value of Ω, being determined by relative fluctuations of the particle interaction with the medium only at neighbouring sites, is independent of the amplitude of the resonant transition and thus also independent of the value of Δ. Therefore, the transition temperature from band motion to incoherent tunneling (which involves, for example, absorption or emission of phonons) is crucially dependent on the particle's mass.

The problem of the tunneling motion of a heavy (with respect to the electron) particle in crystal almost always can be reduced to an underbarrier motion between two nearest wells. Therefore particle dynamics can be described in terms of motion in a two-well potential in the presence of an arbitrary interaction with medium excitations. This picture is characterized by two well-separated time scales: the lifetime τ of a particle in a well and a barrier penetration time π/ν_0, where ν_0 is the vibrational frequency of the particle in the well. For a heavy particle $\nu_0\tau \gg 1$ [3] — *i.e.* the particle spends a long time in a given well and passes through the barrier in a short time.

The pseudo-isotope of hydrogen known as muonium ($\mathrm{Mu} = \mu^+ + \mathrm{e}^-$) is the ideal choice for a diffusing particle, both by virtue of its light mass — almost an order of magnitude smaller than that of hydrogen (protium) itself — and by virtue of the ease with which its mobility can be measured *via* the muon spin relaxation ($\mu\mathcal{SR}$) techniques [4]. The importance of ($\mu\mathcal{SR}$) techniques to experimental studies of quantum diffusion is illustrated by wide variety of crystals, from metals [5] to insulators [6–9], in which both the positive muon (μ^+) and muonium atom show tunneling effects.

Since Δ is small with respect to all other energy parameters in a solid, quantum diffusion is extremely sensitive to crystal imperfections. Therefore, *localization* of the particle often takes place at a relatively low defect concentration, in which case the interaction with excitations *enables* quantum diffusion of the particle, measurement of which can thus provide information on crystal disorder.

Until very recently studies of Mu diffusion have focussed on nearly perfect crystals, in which bandlike motion of Mu persists at low temperatures.

Crystalline defects have been treated mainly as local traps [10] with trapping radii on the order of the lattice constant a. The justification for such an approach was that the characteristic energy of the crystalline distortion, $U(a)$, is usually much less than the characteristic energy of lattice vibrations, Θ. Unfortunately, since it does not take the particle bandwidth Δ into consideration, this comparison turns out to be irrelevant to the problem of particle dynamics, for which the crucial consideration is that Δ is usually several orders of magnitude less than $U(a)$. For example, a typical Mu bandwidth in insulators is on the order of $\Delta \sim$ 0.01-0.1 K [8,11], whereas in insulators $U(a)$ could be as large as 10 K. In metals the mismatch is even more drastic: typical values [$U(a) \sim 10^3$ K *vs.* $\Delta \sim 10^{-4}$ K] differ by about seven orders of magnitude. Under these circumstances, the influence of crystalline defects extends over distances much larger than a. If the "disturbed" regions around defects overlap sufficiently, complete particle localization can result. An understanding of the possible mechanisms of particle localization and delocalization in crystals due to interactions with crystalline defects and lattice excitations is very important in the context of quantum diffusion phenomena.

In this paper we review our recent results on Mu quantum diffusion in cryocrystals. We would concentrate mostly on Mu localization and delocalization phenomena at low temperatures. The wide variety of other problems in muonium quantum diffusion could be found in [9].

2. Muonium Spin Dynamics

The effective spin Hamiltonian of muonium in cryocrystals is taken to be of the form [8]

$$\mathcal{H} = hA\,\vec{S}_e\cdot\vec{S}_\mu - g_e\mu_B\vec{S}_e\cdot\vec{H} - g_\mu\mu_\mu\vec{S}_\mu\cdot\vec{H} + h\sum_n \delta\,\vec{S}_e\cdot\vec{S}_n - \sum_n g_n\mu_n\vec{S}_n\cdot\vec{H}\ , \tag{1}$$

where A is the muonium hyperfine (HF) frequency, $\vec{H}$ is the external magnetic field and the $\vec{S}$, g and μ terms are respectively the spins, g-factors and magnetic moments of the various particles. The summations are over all nearby nuclei. The nuclear hyperfine interaction (NHI) between the muonium electron and neighbouring nuclear dipoles is characterised by the frequency δ. The NHI term is represented as isotropic in Eq. (1) and so may represent either an average magnetic dipole interaction, in a local field approximation, or a contact interaction, in the event that the muonium

electron's wavefunction overlaps with the surrounding nuclei. If muonium and hydrogen occupy equivalent lattice sites, the NHI frequency for nuclei adjacent to muonium is expected to be only slightly different (due to zero point motion) from the value for those adjacent to interstitial hydrogen (protium) itself, which has been measured by ESR (see, for example [12]). It is this interaction which sets the timescale for muon spin relaxation.

Qualitatively, modulation of the nuclear hyperfine interactions results in relaxation of the muonium electron spin, which in turn leads to depolarization of the muon spin *via* the muonium hyperfine interaction.

In transverse field, the relaxation rate T_2^{-1} of the muonium precession signal has a simple form in two limits: if muonium "hops" from site to site at a rate τ_c^{-1} which is much larger than the NHI frequency δ (*fast hopping* limit), then the transverse relaxation rate is given by $T_2^{-1} \approx \delta^2 \tau_c$, which is proportional to the effective width of the local field distribution due to nuclear hyperfine interactions, motionally averaged (hence "narrowed") by fast muonium diffusion with $\tau_c^{-1} \gg \delta$. For very *slow* diffusion ($\tau_c^{-1} \lesssim \delta$) muon spin relaxation takes place on a time scale shorter than τ_c and $T_2^{-1} \approx \delta$. (For this reason, the parameter δ is sometimes referred to as the "static width" due to NHI.) Slow muonium dynamics cannot, therefore, be studied by transverse field measurements.

The interpretation of longitudinal field (LF) measurements of the muonium spin relaxation rate (T_1^{-1}) is based on the notion that the nuclear hyperfine interactions may be treated as an effective magnetic field acting on the muonium electron. Muonium diffusion causes fluctuations of this effective field which induce transitions between the coupled spin states of the electron and muon. The resultant muon depolarization is revealed in the forward-backward asymmetry of the muon decay. Such measurements allow values of τ_c^{-1} and δ to be determined independently [13]. A general expression involves various transitions between the coupled spin states [14] but a reasonable approximation is obtained by assuming dominance of the lowest frequency transition (within the muonium triplet spin states), leading to the expression

$$T_1^{-1} = \frac{2\delta^2 \tau_c}{1 + \omega_{Mu}^2 \tau_c^2} , \tag{2}$$

where $\omega_{Mu} = \gamma_{Mu} H$ is the muonium intra-triplet transition frequency in the magnetic field ($\gamma_{Mu}/2\pi = 1.4012$ MHz/G). This approach is restricted to the limit of relatively high longitudinal fields, however, since the effective magnetic field approximation is valid only if $\gamma_e H \gg \delta$, where γ_e is the electron gyromagnetic ratio. Moreover, in the limit of slow muonium hopping

and high magnetic field, T_1^{-1} is generally too low [see Eq. (2)] to be measured by the standard μSR technique. Thus high LF measurements, which are very sensitive to muonium dynamics in the fast fluctuation regime, are rather ineffective for the study of very slow dynamics.

Zero field (ZF) and weak longitudinal field (wLF) measurements turn out to be much more sensitive to slow muonium dynamics, at least in the case where the spin response is determined by dipolar interactions with neighbouring nuclei. This is due primarily to the fact that these techniques involve the *full* dipolar Hamiltonian rather than just the *secular* part (as is adequate for the transverse field technique; see, for example, [15]). A classical treatment [16] gives an analytical expression for the time evolution of the muon polarization function in zero field, known as the Kubo-Toyabe function: for a Gaussian distribution of static local fields, with second moment $\propto \Delta^2$,

$$P(t) = \frac{1}{3} + \frac{2}{3}\left(1 - \Delta^2 t^2\right) \exp\left(-\frac{1}{2}\Delta^2 t^2\right) . \tag{3}$$

An important feature of Eq. (3) is the "1/3 tail" which, roughly stated, reflects the fact that 1/3 of the muon polarization is, on average, aligned parallel to the local field while 2/3 is transverse to the local field and thus precesses. Although this function [16] was first adopted and experimentally confirmed for μ^+ spin relaxation [17], it is equally applicable for the triplet state of muonium, which can be treated in low magnetic field as one particle with spin $S = 1$. Very slow diffusion, in which the muonium atom jumps between sites with uncorrelated arrangements of neighbouring nuclear spins, is manifest in an observable relaxation of this "1/3 tail" [16,17]. A "strong-collision" treatment [17,18] gives a relaxation function in this regime which may be written (for times $t \gg \Delta^{-1}$) as

$$P(t) \approx \frac{1}{3} \exp\left(-\frac{2}{3}\frac{t}{\tau_c}\right) . \tag{4}$$

This expression for $P(t)$, being independent of Δ, may be used for *direct* measurements of very slow muonium hop rates.

In weak longitudinal field the "tail" of the relaxation function which is sensitive to slow dynamics is shifted to earlier times and has an amplitude several times higher than the "1/3 tail" of the zero field function [19]. This makes the wLF technique even more sensitive than ZF for measurements of extremely slow muonium hop rates.

3. Muonium Diffusion in Solid Nitrogen

3.1. Two-Phonon Quantum Diffusion

Studies of the diffusion of hydrogen atoms [20] and μ^+ [19] in metals, as well as Mu diffusion in insulators [7, 21, 22], have convincingly shown the quantum mechanical character of the phenomenon, most clearly seen at low temperatures where the particle hop rate τ_c^{-1} *increases* with *decreasing* temperature T according to the power law $\tau_c^{-1} \propto T^{-\alpha}$, thus manifesting the onset of the coherent process. In metals, coupling to conduction electrons is the dominant scattering mechanism [23] and causes $\alpha < 1$. In insulators, where phonon scattering processes prevail, α is predicted [1,3] to be *7* or *9* at low temperatures where the absorption of single phonons shifts the energy of the diffusing particle too much for tunneling to occur and so two-phonon diagrams (which can leave the energy almost unchanged) are expected to dominate. Surprisingly, the experimental results on Mu diffusion in *ionic* insulators [7, 21] indicate that α is generally close to *3*; this "universal" power-law behaviour with $\alpha \approx 3$ prompted the authors of Ref. [24] to conclude that muonium diffusion is governed by *one*-phonon scattering. On the other hand, in Ref. [11] it was shown that $\alpha \approx 3$ can also be obtained from *two*-phonon scattering processes if the actual phonon spectrum of the ionic crystal is taken into account; unfortunately, that procedure requires introduction of adjustable parameters. The phonon spectrum of solid nitrogen is consistent with the Debye approximation assumed in more *ab initio* theories, which may thus be tested more directly by experiment.

Transverse field measurements in solid nitrogen [22] revealed a strong nonmonotonic temperature dependence of T_2^{-1}. Below about 10 K Mu T_2^{-1} levelled off as it is expected for very slow diffusion ($\tau_c^{-1} \lesssim \delta$) regime giving value of NHI frequency $\delta = T_2^{-1}$. Therefore, T_1^{-1} measurements were done to study slow Mu hop rates regime (see above). In longitudinal fields the observed relaxation is attributed entirely to the muonium fraction, as the diamagnetic complex in solid nitrogen is known [25] to be the static $N_2\mu^+$ ion, whose relaxation rate is about 0.1×10^6 s^{-1} [26] — far slower than was observed in experiment. Other possible relaxation mechanisms were also ruled out [8].

Figure 1 shows the temperature dependence of T_2^{-1} in transverse field and T_1^{-1} for several values of longitudinal field for Mu in solid nitrogen. At temperatures above 15 K, where $\omega_0 \tau_c \ll 1$, T_1^{-1} becomes independent of field and equal to T_2^{-1}. From Eq. (2) we get the well-known [15] relation for fast diffusion ($\delta \tau_c \ll 1$) and low field ($\omega_0 \tau_c \ll 1$):

$$T_1^{-1} = 2\delta^2 \tau_c = T_2^{-1}. \tag{5}$$

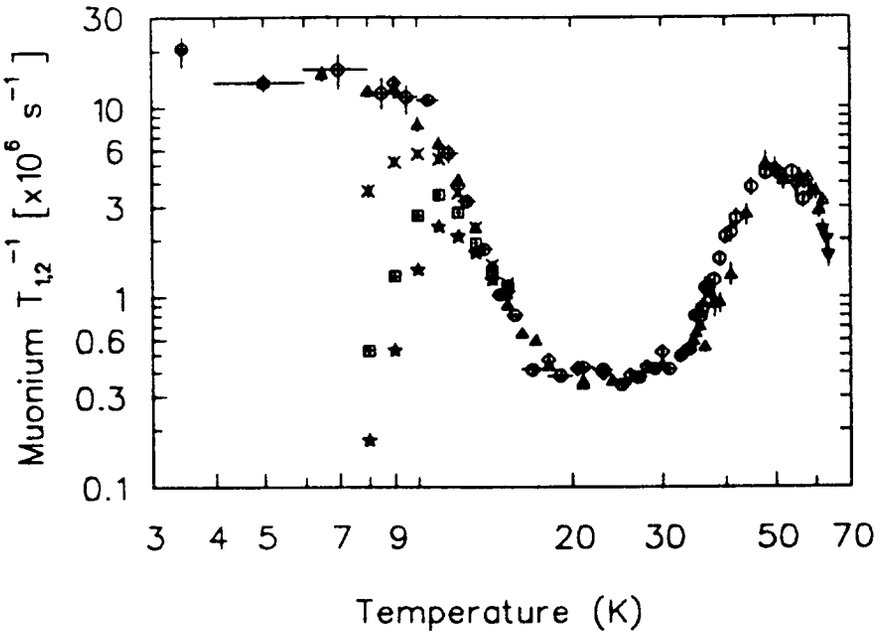

Fig. 1: Muonium relaxation rates in ultra high purity solid N_2 in weak transverse field [circles, triangles, diamonds and inverted triangles correspond to different samples] and several longitudinal fields [stars: 12 G; squares: 8 G; crosses: 4 G].

The T_1^{-1}-maximum effect (in NMR known as T_1-minimum effect [15]) is clearly seen around 10-11 K for all longitudinal fields. For lower longitudinal field the T_1^{-1} maximum is shifted to lower temperature where τ_c is correspondingly shorter. The T_1^{-1}-maximum condition at $\omega_0\tau_c = 1$

$$T_1^{-1}(\max) = \delta^2/\omega_0 \, . \tag{6}$$

allows unambiguous determination of NFI frequency and produces an absolute calibration of the Mu hop rate. Equation (6) allowed us to determine the parameter δ independently for each longitudinal field; all three values are consistent with the combined result, δ=14.9(0.8) MHz, which in turn is within 7% of the value obtained from transverse field measurements [22] at low T.

Figure 2 presents the temperature dependence of the muonium hop rate τ_c^{-1} in solid nitrogen derived from Eq. (2) and complemented by the transverse field data for $T > 12$ K, where motional narrowing leads to Eq. (5).

For temperatures $T \ll \Theta$ (the Debye temperature) quantum diffusion is

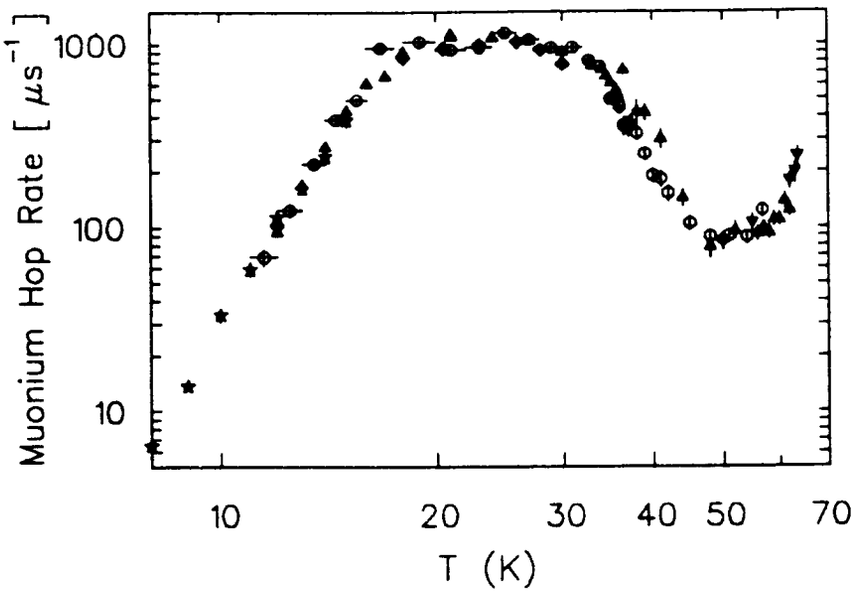

Fig. 2: Temperature dependence of the muonium hop rate in ultra high purity solid N_2. Stars correspond to the combined longitudinal field measurements; circles, triangles, diamonds and inverted triangles correspond to transverse field measurements in different samples.

believed [3] to be governed by two-phonon processes, for which τ_c^{-1} is given by

$$\tau_c^{-1} = \frac{4Z}{3} \frac{\tilde{\Delta}_0^2 \Omega(T)}{\Omega^2(T) + \xi^2}, \tag{7}$$

where Z is the number of the equivalent wells in the nearest coordination sphere and $\tilde{\Delta}_0$ is the renormalized bandwidth for Mu diffusion. The main feature of Eq. (7) is the minimum of $\tau_c(T)$ at $\xi \sim \Omega(T)$.

$$\text{When } \xi < \Omega, \qquad \tau_c^{-1} \propto \frac{\tilde{\Delta}_0^2}{\Omega(T)}; \tag{8}$$

$$\text{but if } \xi \gg \Omega, \text{ then } \tau_c^{-1} \propto \frac{\tilde{\Delta}_0^2 \Omega(T)}{\xi^2}, \tag{9}$$

giving the opposite temperature dependence so that Mu atoms are localized as $T \to 0$.

The only effect of the one-phonon interaction at low temperatures is believed to be an exponential renormalization of the tunneling amplitude [3]. The two-phonon width $\Omega(T)$ is determined by the phonon spectrum of the lattice. In the $T \to 0$ limit only acoustic phonons are important and

$$\Omega(T) \propto T^{7(+2)}. \tag{10}$$

The two additional powers of T appear only in the case of muonium tunneling between absolutely equivalent sites.

In the temperature range $30 < T < 50$ K, the measured Mu hop rate exhibits an empirical temperature dependence $\tau_c^{-1} \propto T^{-\alpha}$ with $\alpha = 7.3(2)$; since, from Eq. (8), $\tau_c^{-1} \propto \Omega^{-1}(T)$, we have $\Omega(T) \propto T^7$ as expected [Eq. (10)]. This is the first experimental confirmation of the T^{-7} dependence of τ_c^{-1} predicted by the two-phonon theory of quantum diffusion [3].

Below about 30 K the Mu hop rate levels off, presumably due to band motion with an estimated [11] renormalized bandwidth of $\tilde{\Delta}_0 \sim 10^{-2}$ K, in agreement with the value deduced from the high-temperature data where one-phonon interactions lead to an enhanced fluctuational preparation of the barrier (FPB) effect [22]. Alternative explanations are given in [8].

This value for the Mu bandwidth in solid nitrogen should be compared with the bandwidth scale $\Delta \sim 10^{-4}$ K obtained for the quantum diffusion of ^{3}He atoms in ^{4}He crystals [27]. Although the former is much larger, the qualitative similarity of these results suggests a common dynamical behaviour for light particles in insulators, as opposed to metals, where different scattering mechanisms lead to quite different impurity dynamics.

Muonium motion slows down again below about 18 K, probably due to the orientational ordering of N_2 molecules. For $T < 18$ K the data in Fig. 2 obey

$$\tau_c^{-1} = \tau_0^{-1} \left(\frac{T}{\Theta}\right)^{\alpha}, \tag{11}$$

with $\Theta = 83$ K (the Debye temperature of nitrogen) [28], $\tau_0^{-1} = 3.6(8) \times 10^{13}$ s^{-1} and $\alpha = 6.7(1)$.

The change in the temperature dependence of the Mu hop rate from a T^7 to a T^{-7} law reflects a crossover from Eq. (8) to Eq. (9). At temperatures below about 18 K gradual Mu localization takes place which reflects a suppression of band motion by static disorder in an imperfect crystal. Subsequent reduction of temperature below 10 K leads to an inhomogeneous quantum diffusion phenomena.

3.2. Inhomogeneous Quantum Diffusion

Most previous experiments on muon diffusion have focussed on normal metals, where coupling of the μ^+ to conduction electrons causes very strong damping, or on very pure insulators, where any effects of crystal imperfections are difficult to observe. Experimental evidence for Mu localization in an imperfect crystal due to suppression of band motion by static disorder was first observed in a solid nitrogen (s-N_2) crystal [8]; however, in that experiment Mu diffusion measurements were restricted to the comparatively high temperature regime governed by pure homogeneous quantum diffusion. At temperatures well below T_0 [where T_0 is determined by the interplay between the particle's energy level broadening $\Omega(T)$, due to coupling with phonons, and the typical difference ξ between energy levels at adjacent tunneling sites, due to static disorder] the observed average *transverse* field relaxation rate T_2^{-1} of muonium should characterize mainly *quasi-localized* Mu atoms in the vicinity of defects. Another fraction of Mu atoms initially located far from impurities or defects should move more rapidly and therefore its muon spin polarization should relax more slowly in transverse field due to motional narrowing. At low temperatures, inelastic scattering by phonons is strongly suppressed [29] and these two Mu fractions remain distinct.

The formation of two independent ensembles of particles is determined by the initial conditions, *i.e.* the locations of Mu atoms with respect to defects just after thermalization. Thus the form of the muon polarization function $P(t)$ at low temperatures will be critically dependent [29] upon the particle bandwidth Δ and the defect concentration n. A distinctive two-component composition of $P(t)$ is a direct manifestation of the crystal's *spatial inhomogeneity* and must be a universal feature of particle diffusion in imperfect crystals whenever static level shifts ξ exceed $\Omega(T)$.

It should be emphasized that a description of the relaxation function in terms of Eq. (2) [a "single τ_c" approximation] is not possible when crystal inhomogeneity causes a spatial distribution of τ_c which we will characterize as $\tau_c(R)$ [where R is the distance to the nearest defect]. This fact was unambiguously experimentally confirmed for Mu diffusion in solid nitrogen [30,31].

Typical μSR time spectra in longitudinal magnetic field $H = 8$ G in s-N_2 at low temperatures are shown in Fig. 3. At temperatures above about 10 K, excellent fits to the data were obtained using expression (2), which assumes that *all* Mu atoms diffuse at the same rate for their entire lifetimes. However, below 10 K it was impossible to fit experimental spectra using a

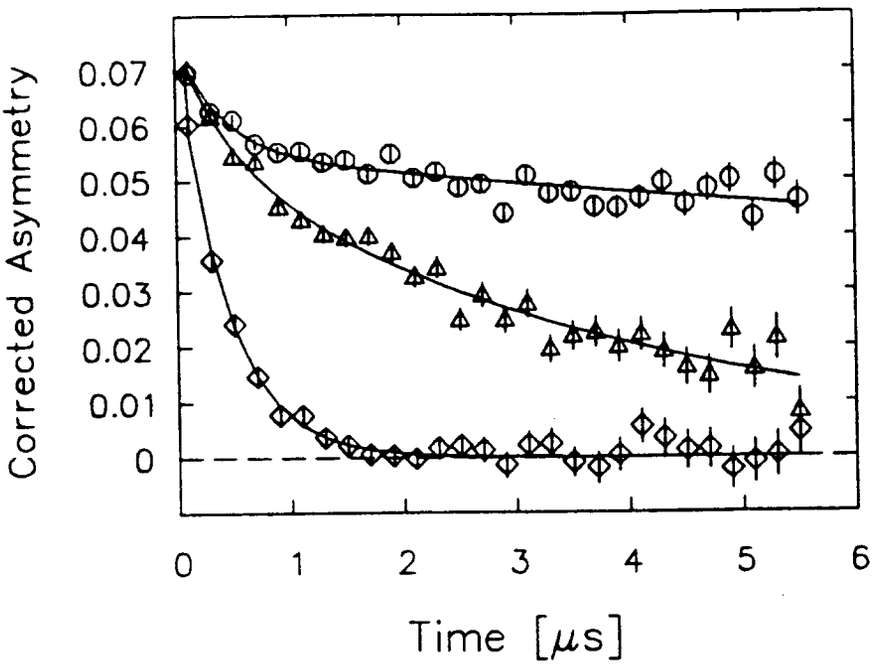

Fig. 3: Muon spin relaxation spectra for muonium in solid nitrogen in a longitudinal field of $H = 8$ Oe at $T = 10$ K (diamonds), 8 K (triangles) and 6 K (circles). Note the presence of two components in the relaxation function at low temperatures.

single exponential relaxation function (2). Figure 3 clearly shows that at low temperatures the polarization function consists of at least two exponential terms. At temperatures below about 8 K a large, almost non-relaxing component (on the μSR time scale) was observed. This component corresponds to an almost static part of the Mu ensemble. A multi-component $P(t)$ is clear evidence for the spatial inhomogeneity of the crystal; muon diffusion experiments in superconducting Al with impurities also show a multi-component $P(t)$, probably due to inhomogeneous diffusion [32].

Experimental time spectra were compared with the simplest possible two-component expression

$$A(t) = A_F \exp(-T_{1_F}^{-1} t) + A_S \exp(-T_{1_S}^{-1} t), \tag{12}$$

where A_F and A_S are the asymmetries (amplitudes) of the fast- and slow-relaxing components and $T_{1_F}^{-1}$ and $T_{1_S}^{-1}$ are their respective relaxation rates. Figure 4 shows the temperature dependences of these asymmetries (a) and

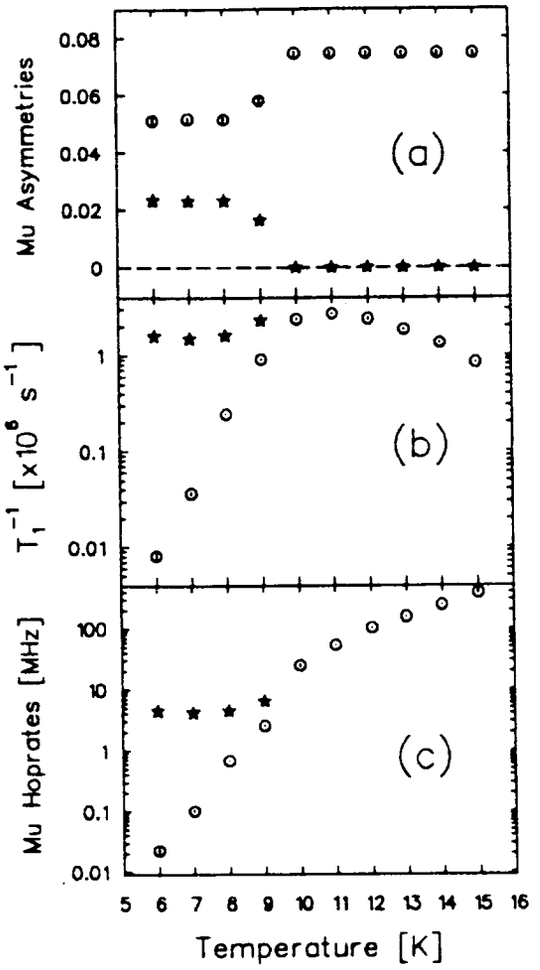

Fig. 4: Temperature dependence of slow-relaxing (circles) and fast-relaxing (stars) muonium signals in solid nitrogen: (*a*) slow (A_S) and fast (A_F) muonium asymmetries (amplitudes); (*b*) slow ($T_{1_S}^{-1}$) and fast ($T_{1_F}^{-1}$) longitudinal relaxation rates; (*c*) slow ($\tau_{c_S}^{-1}$) and fast ($\tau_{c_F}^{-1}$) Muon spin relaxation spectra for muonium in solid nitrogen in a longitudinal field of H = 8 Oe at T = 10 K (diamonds), 8 K (triangles) and 6 K (circles). Note the presence of two components in the relaxation function at low temperatures.

relaxation rates (b) obtained by fitting expression (12) to the data. Above 10 K there is no measurable fast-relaxing component; the entire Mu polarization can be attributed to the slow-relaxing part of the Mu ensemble. As the temperature is reduced below 10 K, A_S decreases and the fast-relaxing component correspondingly increases, clearly indicating the onset of inhomogeneous Mu diffusion. At lower temperatures both A_S and A_F level off, accounting for about 70% and 30% of the Mu polarization, respectively.

The temperature dependence of T_{1S}^{-1} at low temperatures indicates that the slow component undergoes gradual localization as the temperature is reduced, while the fast-relaxing component has a temperature-independent relaxation rate. At $T = 6$ K, T_{1F}^{-1} exceeds T_{1S}^{-1} by more than two orders of magnitude.

Figure 4(c) displays the temperature dependences of the Mu hop rates for the fast and slow components derived from expression (2) with a fixed value of $\delta = 14.9(0.8)$ MHz obtained from T_1^{-1}-maximum conditions [8]. Above about 9 K, Mu exhibits quantum tunneling with a characteristic $\tau_c^{-1} \propto T^7$ temperature dependence [8]. Below this temperature the slow component displays strong localization while the fast component shows temperature-independent Mu motion with about two jumps per muon lifetime.

The muonium hop rate is predicted [3] to have the form (7). It should be noted that static level shifts $\xi = \xi(R)$. At low temperatures the phonon width is reduced $[\xi > \Omega(T)]$ and $\tau_c^{-1} \propto \tilde{\Delta}_0^2 [\Omega(T)/\xi^2(R)]$. In this case inhomogeneity of the crystal results in static level shifts $\xi(R)$ causing a spatial distribution of $\tau_c^{-1}(R)$ and thus, through Eq. (2), a distribution of $T_1^{-1}(R)$.

Reduction of the Mu diffusion rate in s-N_2 at low temperatures has been explained [8] in terms of orientational ordering of N_2 molecules in s-N_2 below $T_{\alpha\beta} \approx 36$ K. Heat capacity, thermal expansion and NMR data in s-N_2 all show peculiarities at low temperatures which are attributed to "orientational defects" caused by an anisotropic interaction between N_2 molecules [28]. This is a peculiar intrinsic property of crystalline nitrogen, which can be considered as homogeneous at high temperature but has the properties of a translationally disordered lattice below $T_{\alpha\beta}$. Thus different interstitial lattice sites for the Mu atom which are energetically degenerate at high temperatures become separated by static level shifts $\xi(R)$ at low temperatures due to defects in the molecular orientational ordering; this produces "crystal disorder" for Mu diffusion so that Mu has to overcome energy shifts $\xi(R)$ and the hop rate is decreased according to Eq. (7). This picture is consistent with the behaviour of the slow-relaxing component, while the fast-relaxing component probably represents those Mu

atoms (about 30%) undergoing coherent tunneling which scatter elastically off distorted regions near defects.

3.3. Trapping Phenomena in an Insulators

At low temperatures even weak interactions with defects may be stronger than the inelastic interaction with the environment, leading to effective traps for diffusing particles. As a result, for many years μ^+ and Mu quantum diffusion in crystals was discussed in terms of trapping effects regardless of the temperature range or the nature of the crystal (see, for example, [10] and references therein). In this section we present strong experimental evidence that such trapping effects, which may be dominant in metals [33], can be rather ineffective in insulators at low temperatures.

The trapping rate K in an imperfect crystal is usually expressed as

$$K = 4\pi c n R_T D(R_T), \tag{13}$$

where c is a numerical coefficient on the order of unity, n is the impurity concentration, R_T is trapping radius defined by the condition

$$U(R_T) = T \tag{14}$$

and $D(R_T)$ is the diffusion coefficient [34]. From Eq. (14) one could immediately note that defect potential has rather *long-ranged* character with $R_T \gg a$. In "dirty" insulators (and superconductors [35]) at low temperatures the temperature dependence of $D(R_T)$ is opposite to that in a perfect crystal [see Eq. (7)]. Thus the trapping rate decreases rapidly with temperature, making the trapping mechanism essentially ineffective.

Figure 5 shows the temperature dependence of the transverse relaxation rate T_2^{-1} of muonium in pure s-N_2 (a) and in s-N_2 with 10^{-3} CO impurities (b). When Mu hops rapidly in s-N_2 (causing low values of T_2^{-1} due to dynamical "narrowing"), the Mu atom finds a CO impurity in the N_2+CO crystal and reacts chemically (probably to form the MuCO· radical [36]), which explains the fact that the maximum T_2^{-1} value for Mu in s-N_2+CO significantly exceeds that for static Mu in pure nitrogen where it is determined by the interaction of localized Mu with the nuclear magnetic moments of neighboring N_2 molecules. This chemical reaction is manifest in an exponential relaxation of the Mu polarization, the rate of which is determined by the time required for Mu to approach the CO impurity within a distance a, after which the reaction occurs immediately. This description in terms of chemical reaction controlled by Mu diffusion is almost perfectly analogous to the phenomenology of trapping.

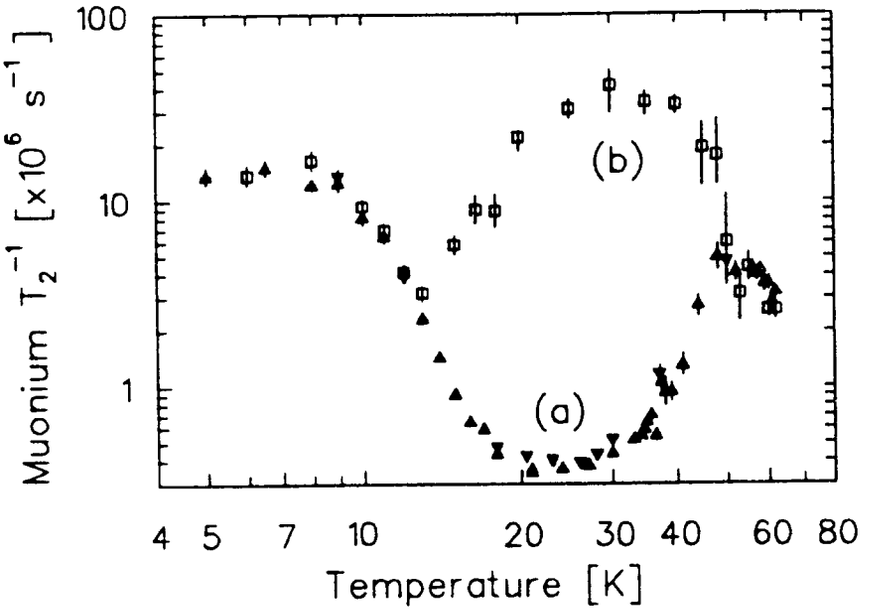

Fig. 5: Temperature dependence of the transverse relaxation rate (T_2^{-1}) of muonium
(a) in pure nitrogen crystals (triangles, two different samples) and
(b) in a crystal of N_2 + 10^{-3} CO.

At high temperatures the clear maximum in T_2^{-1} for Mu in s-N_2+CO marks the crossover from fast to slow Mu diffusion near CO impurities, which in turn reflects the interplay between $\Omega(T)$ and ξ in the denominator of Eq. (7). In this temperature range the strong coupling to phonons allows Mu to overcome the defect potential and move to react with CO. However, the energy shift ξ which the particle has to overcome is much larger close to the defect than far from it, making the Mu hop rate strongly dependent on the distance from the defect.

At low temperatures the suppression of inelastic interactions with the lattice changes Mu diffusion drastically. There is no longer an energy bath from which Mu can gain the energy needed to overcome site energy differences close to CO impurities. Therefore, Mu atoms are stuck (or "frozen") far from impurities, causing a strong reduction of the reaction rate (Mu relaxation rate). Muonium atoms are then effectively excluded from the volumes around the impurities and T_2^{-1} is the same for pure N_2 and N_2+CO crystals, as clearly seen in the experiment (Fig. 5).

Thus the trapping mechanism is shown to be essentially ineffective at low

temperatures in insulators, as demonstrated by our experiment in N_2+CO. It should be noted, however, that in normal metals strong coupling to conduction electrons produces $\Omega(T) \propto T$ [23]. Thus for $\xi < T$ the diffusion process in normal metals is rather *homogeneous* (for $\xi > T$ the particle might be considered as already trapped).

4. Muonium One-Phonon Quantum Diffusion and Localization in Heavy Rare Gas Solids

The tunneling motion of a particle in a solid is often governed by two channels of the interaction with the medium. First channel gives rise to the effect of fluctuational preparation of the barrier (FPB) [37] and characterises the interaction of a particle with barrier fluctuations during the passage through the barrier region. Second channel is due to intrawell interaction and manifests the appearance of the polaron effect (PE) [38].

As long as the diffusing particle is much lighter than the atoms composing the medium, the former will vibrate at a characteristic frequency ν_0 much higher than the typical vibrational frequency of the latter, which is of the order of the crystal's Debye temperature Θ in this case a light interstitial atom will respond almost adiabatically to lattice vibrations, including the quantum zero-point motion (ZPM) of nearby lattice atoms, resulting in an enhanced tunneling probability when the surrounding atoms happen to assume a configuration in which the barrier along the optimal particle path separating the current interstitial site from a neighbouring one is instantaneously lower and/or narrower than on average. This version of FPB applies even at zero temperature and increases the rigid-lattice tunneling bandwidth Δ_0 of the particle to an effective $T = 0$ bandwidth $\Delta = \Delta_0 e^G$ in the absence of other effects (see below). The FPB exponent G is proportional to the mean square fluctuations of the quasiclassical tunneling action and can be expressed conveniently as $G \sim (\delta U_B/\hbar\nu_0)^2$, where δU_B is a typical fluctuation of the barrier height.

The observed value for the bandwidth is also renormalized because of the PE which inevitably occurs in any non-rigid lattice: the interstitial atom causes the surrounding lattice to relax slightly, "digging a hole" for itself and lowering its energy in the current site by E_P relative to that which one would calculate for a perfectly rigid lattice. The combination of self-trapped interstitial and accompanying lattice distortion are commonly referred to as a quasiparticle known as a *small polaron*. The effect of the PE energy shift E_P is to decrease the probability of resonance between the energy of the light atom in its current interstitial site and the energy it would have in an

adjacent site prior to reconfiguration of the lattice distortion. In effect, this *narrows* the tunneling bandwidth, giving $\Delta = \Delta_0 e^{-\phi} e^{G}$ at $T = 0$, where ϕ is another dimensionless parameter describing the reduction of resonant tunneling opportunities due to the PE energy shift. Actually the particle has to wait for the lattice fluctuation which brings the distorted configuration around the initial particle site into the symmetric configuration allowing resonant transition between the sites. Such a fluctuation is very rare if adjacent atoms' displacements δu are large compared with the root mean square ZPM amplitude $\sqrt{\langle u^2 \rangle_0}$. One can estimate the polaron factor in the exponent as $\phi \sim \delta u^2 / \langle u^2 \rangle_0 \sim E_P / \Theta$.

The parameters ϕ and G are related to the displacements of different groups of atoms, so that one might easily imagine cases when $\delta U_B \gg E_P$ — for instance, if the interaction between the particle and a lattice atom is a strong function of the distance between them and the tunneling process leads to their approach. To be more precise, PE and FPB are not completely independent — the PE lattice distortion also alters the average shape and height of the barrier so that, even in the absence of latice ZPM, there would be a PE-induced renormalization of the tunneling bandwidth which we may characterize by a separate temperature-independent dimensionless parameter B, giving a final expression for the tunneling bandwidth [37]

$$\Delta = \left(\Delta_0 e^{B} \right) e^{-\phi} e^{G} \, . \tag{15}$$

Obviously one can at best measure Δ itself, so it is only through theoretical estimates that one can form opinions about the relative importance of ϕ, which decreases the tunneling rate, G, which increases it, and B, which could do either. At present we are not aware of any first-principles calculations of Δ_0 which are precise enough even to determine the overall sign of $(\Delta - \Delta_0)/\Delta$.

At finite temperatures, real phonons begin to affect the tunneling process. However, in the temperature range $T \ll \Theta$, where the average amplitude of lattice vibrations is hardly changed compared to that due to ZPM, one can describe the particle dynamics in the framework of standard kinetic equations assuming a constant value for the tunneling matrix element [1]. The remarkable phenomenon of crossover from coherent band motion to incoherent hopping [3, 8] takes place in this temperature range where Δ is essentially unchanged. Only at very high temperatures $T \sim \Theta$ do the effective vibrational amplitudes of individual lattice atoms begin to have *rms* values significantly larger than those attributable to ZPM, at which point the effects due to FPB acquire temperature dependences.

The PE, which is likely to have a larger effect on the coherent bandwidth at $T = 0$, should become less important at high T (see below), whereas FPB effects increase and become dominant for $T > \Theta$. The mean square vibration amplitude increases linearly with T at high temperature ($\langle u^2 \rangle \approx \langle u^2 \rangle_0 \, T/\Theta$) and so does the mean square fluctuation of the barrier height. Clearly, as the temperature increases so does the probability of "easy" tunneling opportunities as lattice atoms fluctuate away from the particle trajectory connecting adjacent sites. Thus we find $G(T) \approx G(0) \, T/\Theta$. On the other hand, large amplitude vibrations simply wash out the effect of lattice distortion around the particle because all lattice configurations are equally accessible at high T. Substituting $\langle u^2 \rangle_0 \rightarrow \langle u^2 \rangle$ in the earlier expression for the polaron exponent, we arrive at the well known result that "polaron narrowing" disappears as $\exp(-E_P/4T)$ [38].

The full expression (including all PE and FPB effects) for the tunneling hop rate τ_c^{-1} is thus [3,11]

$$\tau_c^{-1} = \frac{2(\Delta_0 e^B)^2 \sqrt{\pi}}{\sqrt{(E+\gamma)T}} \exp\left[-\frac{E}{T} + \frac{T}{E_B} - \frac{T\xi_B^2}{16(E+\gamma)}\right] . \tag{16}$$

where the "activation" energy E is directly related to the polaron shift ($E = E_P/4$) and E_B can be approximated by $E_B \sim \Theta/G(0)$. The last term in the exponent describes a mixing of the two effects because, as mentioned above, in the presence of lattice distortions the average barrier does not correspond to the rigid lattice value. The last two terms in Eq. (16) have exactly the same linear temperature dependence and are therefore experimentally indistinguishable; nevertheless, specific choice of the medium under investigation may allow one to separate FPB and PE using Eq. (16).

The PE is sure to be much weaker in insulators than the electronic version in metals [23], which can lead to complete localization of the tunneling particle in a crystal despite translational symmetry. The FPB effect, on the other hand, may become dominant for the case of phonon-coupled neutral atoms in insulators, whereas FPB is less significant for electron-coupled charged particles in metals [3].

The conditions under which one can experimentally separate the effects of FPB from PE are therefore rather specific: One should study a light neutral atom diffusing in a "soft" insulating crystal composed of heavy atoms, ensuring $\nu_0 \gg \Theta$ and minimizing any competing PE. One should study the temperature dependence of the tunneling rate τ_c^{-1} at high temperatures $T > \Theta$, where the thermal FPB effect is strongest. One must not, however, approach the temperature $T^* \sim \nu_0$ at which classical over-barrier hopping

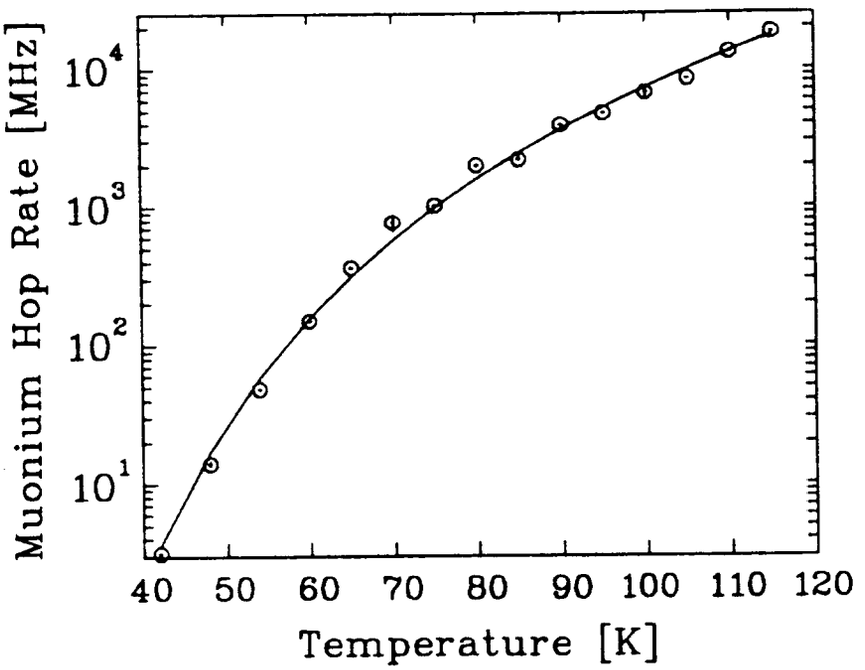

Fig. 6: Temperature dependence of the Mu hop rate τ_c^{-1} in natural s-Xe.

sets in [39]. The region $\Theta < T < T^*$ is most sensitive to one-phonon quantum diffusion [3] and will be most likely to reveal FPB effects. This emphasizes the need for a medium with a low Debye temperature, *e.g.* a Van der Waals crystal such as solid xenon and krypton, the heaviest solids in which the ideal light interstitial atom for such a study — muonium — has ever been observed [9,40–42].

4.1. Muonium Diffusion in Solid Xenon

As natural Xe possesses of about 45% of isotopes with the nonzero nuclear magnetic moments, muonium T_2^{-1} turned out to be too high to extract Mu hop rate temperature dependence [41]. Therefore, high longitudinal field technique was applied for this purpose [9]. Measurements in natural Xe and ^{136}Xe clearly showed that below about 115 K Mu relaxation T_1^{-1} is due to Mu dynamics in Xe lattice. Above this temperature Mu relaxation is believed to be due to some other reason.

Observation of T_1^{-1} maxima in different magnetic fields clearly showed that Mu atom undergoes gradual localization with lowering temperature in solid Xe. Figure 6 presents the temperature dependence of the Mu hop rate

in natural xenon.

Several arguments arose against a classical over-barrier hopping model. First, it gave a poor fit to the experimental $\tau_c^{-1}(T)$ data, which show an apparent change in the effective activation energy near $T = \Theta$; this cannot be attributed to classical hopping "taking over" from quantum tunneling above Θ, because the slope of the T-dependence *decreases* above $T \approx \Theta$, whether one plots the data as in Fig. 6 or as an Arrhenius plot. Second, the apparent pre-exponential factor is at least two orders of magnitude smaller than ν_0. Finally, a simple estimate of the temperature T^* at which quantum diffusion is expected to give way to classical diffusion gives $T^* \sim 200\ \mathrm{K} \gg \Theta$.

Analysis of the experimental data using PE or FPB effects separately and using full expression (16) showed that addition of FPB effect into fitting program improve χ^2 parameter slightly. Measurements of muonium tunneling kinetics in solid xenon [9] revealed that both effects could be important at temperatures comparable with the Debye temperature of the crystal, Θ. However, additional experiments, especially at low temperatures, are required to determine precise temperature regions were FPB or PE prevail.

An unprecedented variation of the muonium hop rate over 4 decades in solid Xe clearly demonstrated the tendency of muonium atoms to become localized at low temperatures. However, interpretation of the longitudinal field data at low temperatures in solid Xe (*i.e.* the regime of muonium localization) is hampered by a rather complicated multiexponential form of the muonium spin relaxation function. A strong hyperfine interaction between the muonium electron and the xenon nuclei (almost half of which have non-zero magnetic moments) hinders transverse field [41] and zero field $\mu\mathcal{SR}$ measurements at low temperatures. In consequence, muonium localization and slow tunneling have not previously been studied experimentally in rare gas solids.

4.2. Muonium Localization in Solid Krypton

In this section we describe the first experimental study of muonium localization at low temperature in a rare gas crystal, presenting data for solid krypton [42]. This study is made possible by the low natural abundance of the sole isotope (^{83}Kr) to carry a magnetic moment: distinctive zero field and weak longitudinal field $\mu\mathcal{SR}$ spectra characterise the extremely slow muonium dynamics in the Kr lattice. We present the first observation of Kubo-Toyabe relaxation for a paramagnetic atom. The use of both zero field and weak longitudinal field techniques allows the determination of Mu hop rates two orders of magnitude slower than the inverse μ^+ lifetime, in a regime previously inaccessible.

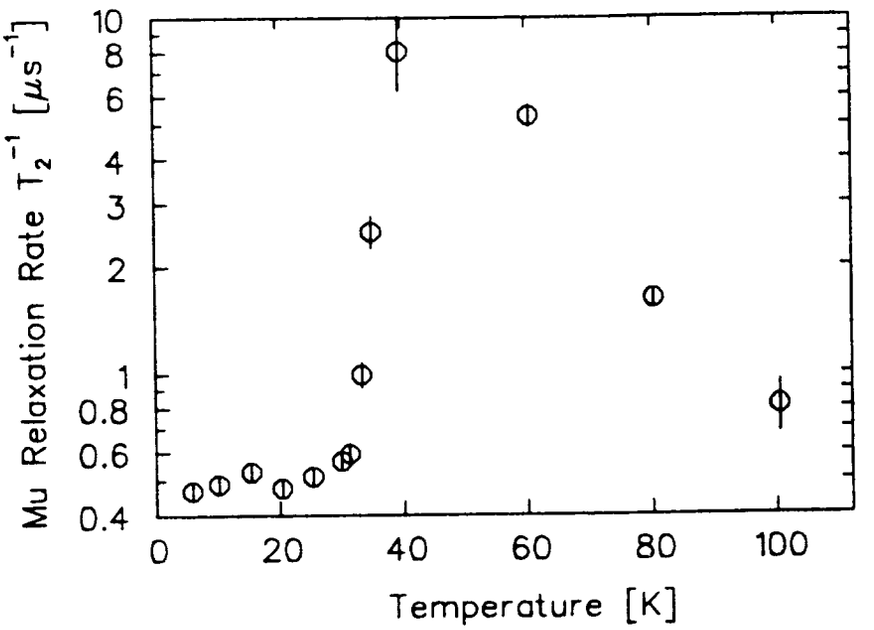

Fig. 7: Temperature dependence of the muonium relaxation rate T_2^{-1} in solid Kr in a transverse magnetic field $H = 2\ G$.

Figure 7 presents the temperature dependence of the muonium transverse relaxation rate T_2^{-1} in condensed krypton, extracted from the data by fitting single-exponential relaxation functions. The main mechanism of muonium relaxation in solid Kr undoubtedly involves dipolar or hyperfine interactions between the Mu spin and ^{83}Kr nuclei (natural abundance 11.55%). The increase in T_2^{-1} upon lowering the temperature from 100 K to 40 K may be explained by a slowing down of the muonium diffusion in solid Kr. It would be tempting to explain the characteristic maximum and abrupt drop in T_2^{-1} at about 40 K in terms of motional averaging of these interactions due to fast muonium diffusion, which would imply a rather abrupt onset of quantum tunneling at low temperatures. This drop, however, is accompanied by a drop in the amplitude of the TF precession signal from 0.0671(5) to 0.0395(5), corresponding to a reduction of the apparent muonium fraction to 58.9% of its value at higher temperatures. This behaviour cannot be explained by the onset of a fast diffusion regime. It can, on the other hand, be explained in terms of the isotopic composition of krypton and the consequent fact that not all crystallographically equivalent sites have equivalent local nuclear magnetism. Those muonium atoms which localize at

sites having nearest neighbour ^{83}Kr nuclei experience strong nuclear hyperfine interactions and are rapidly and completely depolarized, whereas those which localize at sites with spinless nearest neighbours (experiencing much smaller, and predominantly dipolar, local fields from remote ^{83}Kr nuclei) exhibit a relatively slowly damped precession signal. An abrupt decrease of T_2^{-1} with decreasing temperature, accompanied by a simultaneous reduction in the precession amplitude, can therefore be explained by *localization* of the *whole* muonium fraction in solid Kr at low temperatures. Above about 35 K, the muonium atoms become *delocalized* and the entire Mu ensemble experiences close-range interactions with ^{83}Kr nuclei in the course of diffusion through the lattice, leading to the stepwise increase in $T_2^{-1}(T)$. If this explanation is correct, the nature of the muonium localization site in the Kr lattice can be determined by comparison of the muonium fraction which remains observable at low temperature (58.9%) with the probability of finding sites of different symmetry having spinless nearest neighbours. Assuming a uniform random distribution of ^{83}Kr, the probability that a tetrahedral site should have all four near nighbours spinless is 61.2%, while the probability that an octahedral site should have all six nearest neighbours spinless is 47.9%. It seems most likely, therefore, that muonium occupies the tetrahedral interstitial position in the Kr lattice. A substitutional position can reasonably be discounted, in view of the very low probability that all twelve nearest neighbours should be spinless. (This contrasts with the situation for co-deposited hydrogen atoms, which do apparently take up the substitutional position [12] — the NHI frequencies in the vicinity of muonium and hydrogen atoms in solid krypton could therefore be considerably different, as our longitudinal field measurements reveal; see below.)

In order to confirm the hypothesis of muonium localization at low temperatures, we undertook zero field measurements at $T = 20.3$ K. Figure 8 presents the time evolution of the muon polarization (circles) and shows that it exhibits a relaxation function of the Kubo-Toyabe type [see equation (3)]. This can only be attributed to essentially static interstitial muonium. The line drawn through the experimental points represents a best fit to a "dynamicized" version [19, 43] of Eq. (3), taking into account both sites with nearest neighbour ^{83}Kr nuclear spins and those without. The former contribute a Kubo-Toyabe function with its characteristic minimum shifted to very early times (invisible in the dead time of the $\mu\mathcal{SR}$ spectrometer); the "1/3 tail" of this component constitutes a baseline to the Kubo-Toyabe function actually observed, which is characteristic of the local field distribution from more distant dipolar nuclei at the latter type of sites whose immediate neighbours are spinless. The rather long correlation time τ_c is

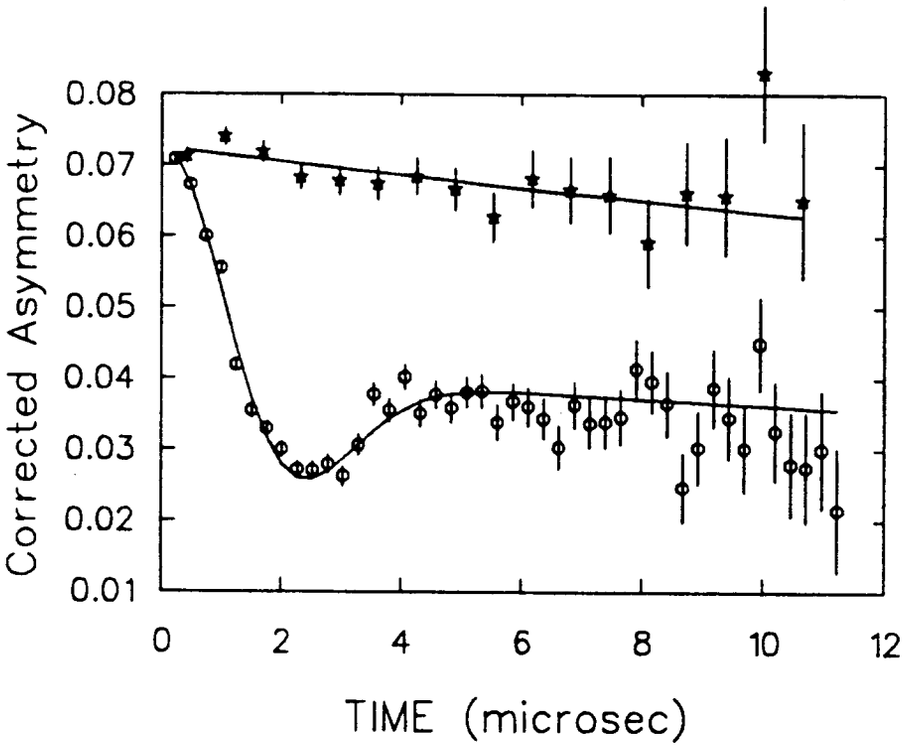

Fig. 8: Time dependence of the muonium polarization in solid Kr in zero magnetic field (circles) and in a weak longitudinal magnetic field $H = 5\ G$ (stars). Note the Kubo-Toyabe form of the muon polarization function in zero magnetic field.

assumed to be the same for both types of sites, since they are electrostatically identical. For comparison, Fig. 8 also shows the muonium polarization function in solid Kr for a longitudinal field of 5 G (stars).

Very slow muonium diffusion rates were measured both in zero field and in a *very* weak longitudinal field (0.2 G). Both the hop rate τ_c^{-1} and the NHI frequency δ_{nnn} (with next nearest neighbours) were determined by simultaneously fitting zero field and weak longitudinal field data to corresponding dynamical gaussian Kubo-Toyabe relaxation functions [19, 43] with $\Delta \equiv \delta_{nnn}$ [recall Eq. (3)]. At temperatures above about 30 K, the high longitudinal field technique was applied to measure the faster hop rates. The temperature dependence of T_1^{-1} in different values of applied field is shown in Fig. 9. Between about 30 K and 55 K, the $T_1^{-1}(T)$ data can safely be interpreted in terms of muonium diffusion, as the variation of T_1^{-1} with magnetic field is consistent with a diffusion model [13]. Above about

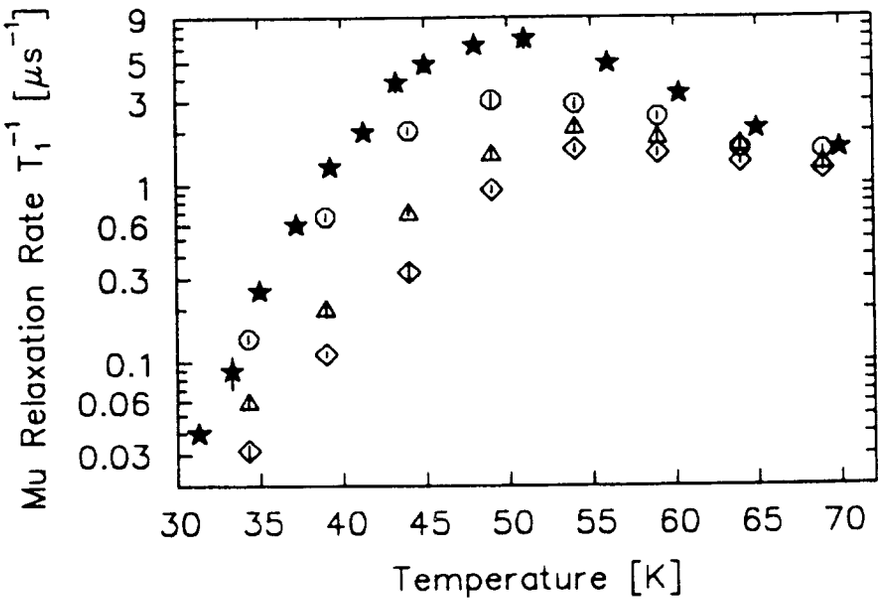

Fig. 9: Temperature dependence of the muonium relaxation rate T_1^{-1} in solid Kr in several longitudinal magnetic fields: 40 G (stars), 60 G (circles), 120 G (triangles) and 180 G (diamonds). Note the T_1 minima (T_1^{-1} maxima) around 50 K.

55 K, it appears that the relaxation is no longer governed by local nuclear hyperfine interactions; a similar change of regime has also been observed in solid natural xenon and solid ^{136}Xe [9].

Clear T_1^{-1} maxima are seen around 55 K. For lower LF the T_1 minima are shifted to lower temperatures, indicating a gradual decrease of muonium mobility with decreasing temperature, which is consistent with the increasing localization seen in zero and weak longitudinal fields data. The motional correlation time τ_c and NHI frequency δ_{nn} (with nearest neighbours) were determined by simultaneous fitting of the LF-$\mu\mathcal{SR}$ spectra taken at several fields to a general expression [13]. The positions of the T_1 minima for several fields provided an absolute calibration for both parameters [15].

Muonium NHI frequencies with nearest and next-nearest neighbours were determined to be δ_{nn} = 55(5) MHz (from longitudinal field data) and δ_{nnn} = 0.67(6) MHz (from zero and weak longitudinal fields data), respectively. This difference of almost two orders of magnitude between nearest and next-nearest neighbour interactions with ^{83}Kr nuclear moments suggests that these interactions are, respectively, contact and dipolar in character. The

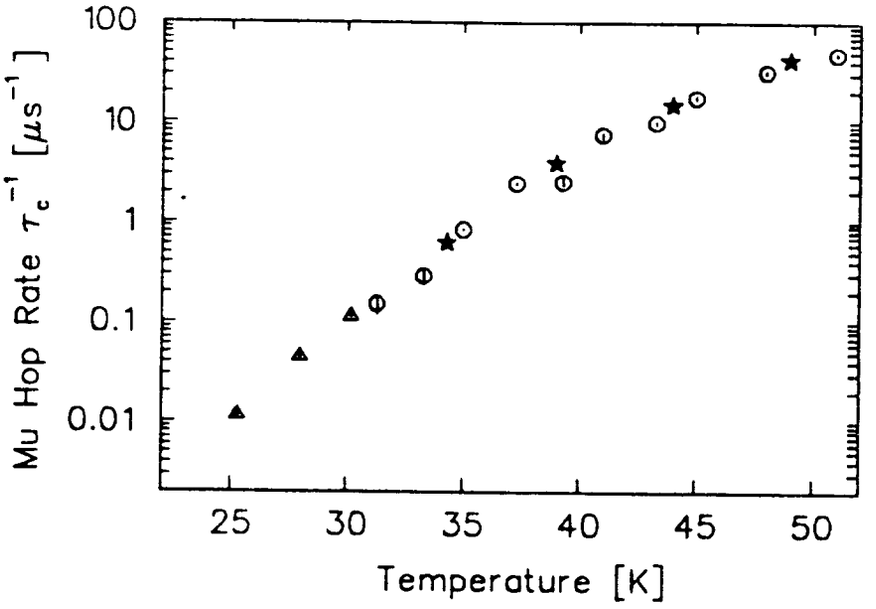

Fig. 10: Temperature dependence of the muonium hop rate derived from simultaneous fits to zero and weak longitudinal fields data (triangles, ISIS data) and high longitudinal field data (circles, ISIS data; stars, TRIUMF data).

large value for the nearest neighbours is at the upper limit of values encountered for purely dipolar interactions; we therefore suspect that the muonium wavefunction actually overlaps onto neighbouring krypton nuclei to give a contact term. Apart from this somewhat surprising result, treatment of the zero field data with the Kubo-Toyabe relaxation function is almost certainly justified, since $\Delta \equiv \delta_{nnn}$ surely has a dipolar origin.

The temperature dependence of the muonium hop rate in solid Kr derived from simultaneous fits to zero and weak longitudinal fields data (triangles) and high longitudinal fields data (circles, measured at ISIS, and stars, measured at TRIUMF) are shown on the Fig. 10. The hop rate values obtained show very good agreement between high longitudinal field data and zero and weak longitudinal fields data around 30 K. The low-temperature results represent the slowest interstitial hop rates ever measured by $\mu\mathcal{SR}$, either for μ^+ or for neutral muonium. Below about 25 K, the muonium τ_c is some two orders of magnitude longer than the muon lifetime. Above 25 K, the muonium hop rate shows an increase of almost 4 orders of magnitude with rising temperature.

It is known that one-phonon quantum diffusion [9] takes over from the low-temperature two-phonon quantum diffusion [8] above a few tenths of the Debye temperature [3]. As the Debye temperature for solid Kr is $\Theta = 72$ K [28], muonium diffusion in the above-mentioned temperature range in solid Kr is expected to be governed by the one-phonon quantum mechanism. The alternative possibility of classical over-barrier hopping, with the Arrhenius dependence

$$\tau_c^{-1} = \tau_0^{-1} \exp(-E/T) \tag{17}$$

requires the pre-exponential factor τ_0^{-1} to be comparable with ν_0. Fitting the experimental $\tau_c^{-1}(T)$ dependence for 25 K$< T <$55 K to Eq. (17) gave a pre-exponential factor $\tau_0^{-1} = 1.6(3) \times 10^{11}$ s^{-1}, which is at least two orders of magnitude less than ν_0. Classical diffusion may therefore be eliminated as a possible mechanism of muonium diffusion in solid Kr at temperatures below 55 K. Analysis of the diffusion rate in this region showed that both the PE and FPB effects should be taken into account in this material. Precise determination of the parameters for one-phonon muonium diffusion in solid krypton, however, requires more detailed measurements in high longitudinal fields.

5. Summary

Studies of muonium diffusion in cryocrystals have supported basic points of current quantum diffusion theory [3,29]. Our experiments reveal strong particle *localization* at low temperatures in *all* studied cryocrystals. This result is fundamentally different from Mu diffusion in pure ionic crystals and compound semiconductors [7,21]. The nature of this difference is not yet understood. Further studies, especially in cryocrystals with deliberately inserted impurities, would probably solve this intriguing problem.

6. Acknowledgments

This work was supported by the Canadian Institute for Advanced Research, the Natural Sciences and Engineering Research Council and (through TRIUMF) the National Research Council of Canada. Support of the International Science Foundation (through Grant N9D000), INTAS Foundation (through Grant 94-3394), Royal Society of the United Kingdom (through RS Award) and Prof. S.T. Belyaev is acknowledged by one of us (VS). We would like to thank S.F.J. Cox and N.V. Prokof'ev for helpful discussions.

References

[1] A.F. Andreev and I.M. Lifshitz, *Sov.Phys.JETP* **29**, 1107 (1969).

[2] R.A. Guyer and L.I. Zane, *Phys.Rev.* **188**, 445 (1969).

[3] Yu. Kagan and N.V. Prokof'ev, "Quantum Tunneling Diffusion in Solids", in *Modern Problems in Condensed Matter Science*, eds. A.J. Leggett and Yu.M. Kagan (North-Holland, 1992).

[4] A. Schenck, *Muon Spin Rotation: Principles and Applications in Solid State Physics*, (Adam Hilger, Bristol, 1986); S.F.J. Cox, *J. Phys.* **C20**, 3187 (1987); J.H. Brewer, "Muon Spin Rotation/Relaxation/Resonance", in *Encyclopedia of Applied Physics*, in press (1995).

[5] G.M. Luke *et al.*, *Phys. Rev.* **43**, 3284 (1991).

[6] R.F. Kiefl *et al.*, *Phys. Rev. Lett.* **62**, 792 (1989).

[7] R. Kadono, *Hyperfine Int.* **64**, 615 (1990).

[8] V. Storchak *et al.*, *Phys. Rev. Lett.* **72**, 3056 (1994).

[9] V. Storchak, J.H. Brewer, and G.D. Morris, *Hyperfine Int.*, **85**, 31 (1994).

[10] R. Kadono, in *Perspectives in Meson Science*, ed. T. Yamazaki, K. Nakai and K. Nagamine, (North-Holland, Amsterdam), p.113, 1992.

[11] Yu.M. Kagan and N.V. Prokof'ev, *Phys. Lett.* **A150**, 320 (1990).

[12] S.N. Foner *et al.*, *J. Chem. Phys.* **32**, 963 (1960).

[13] M. Celio, *Helv. Phys. Acta* **60**, 600 (1987); H.K. Yen, M.Sc. thesis, University of British Columbia, 1988 (unpublished).

[14] S.F.J. Cox and D.S. Sivia, *Hyperfine Int.* **87**, 971 (1994).

[15] C.P. Slichter, *Principles of Magnetic Resonance* (Springer-Verlag, 1980).

[16] R. Kubo and T. Toyabe, in *Magnetic Resonance and Relaxation*, ed. by R. Blinc (North-Holland, Amsterdam, 1966), p.810.

[17] R.S. Hayano *et al.*, *Phys. Rev. B* **20**, 850 (1979).

[18] R. Kubo, *J. Phys. Soc. Jpn.* **9**, 935 (1954).

[19] G.M. Luke *et al.*, *Phys. Rev.* **43**, 3284 (1991)

[20] D. Steinbinder *et al.*, *Europhys. Lett.* **6**, 535 (1988).

[21] J.W. Schneider *et al.*, *Phys. Rev. Lett.* **68**, 3196 (1992).

[22] V. Storchak *et al.*, *Phys. Lett.* **A182**, 449 (1993).

[23] J. Kondo, *Physica* **125B**, 279 (1984); **126B**, 377 (1984); K. Yamada, *Prog. Theor. Phys.* **72**, 195 (1984).

[24] P.C.E. Stamp and Chao Zhang, *Phys. Rev. Lett.* **66**, 1902 (1991).

[25] V. Storchak *et al.*, *Chem. Phys. Lett.* **200**, 546 (1992).

[26] B.F. Kirillov *et al.*, *Hyperfine Int.* **65**, 819 (1990).

[27] M.G. Richards *et al.*, *J. Low Temp.Phys.* **24**, 1 (1976); V.A. Mikheev *et al.*, *Fiz. Nizk. Temp.* **3**, 386 (1977) [*Sov. J. Low Temp. Phys.* **3**, 186 (1977)].

[28] *Cryocrystals*, eds. B.I. Verkin and A.F. Prikhotko (Naukova Dumka, Kiev, 1983).

[29] N.V. Prokof'ev, *Hyperfine Interactions*, **85**, 31 (1994).

[30] V. Storchak *et al.*, *Hyperfine Int.*, **85**, 103 (1994).

[31] V. Storchak *et al.*, *Phys. Rev. Lett.*, to be published.

[32] E. Karlsson *et al.*, to be published.

[33] O. Hartmann *et al.*, *Phys. Rev.* **B37**, 4425 (1988).

[34] T.R. Waite, *Phys. Rev.* **107**, 463 (1957); K. Schroder and K. Dettmann, *Z. Phys.* **B22**, 343 (1975).

[35] Yu.M. Kagan and N.V. Prokof'ev, *Phys. Lett.* **A159**, 289 (1991).

[36] S.F.J. Cox *et al.*, *Hyperfine Interactions* **65**, 773 (1990).

[37] Yu. Kagan and M.I. Klinger, *Zh. Eksp. Teor. Fiz.* **70**, 255 (1976) [*Sov. Phys. JETP* **43**, 132 (1976)].

[38] C.P. Flynn and A.M. Stoneham, *Phys. Rev. B* **1**, 3966 (1970).

[39] I.M. Lifshitz and Yu.M. Kagan, *Zh. Eksp. Teor. Fiz.* **62**, 385 (1972) [*Sov. Phys. JETP* **35**, 206 (1972)].

[40] R.F. Kiefl *et al.*, *J. Chem. Phys.* **74**, 308 (1981).

[41] V. Storchak *et al.*, *Phys. Lett. A* **32**, 77 (1992).

[42] V. Storchak *et al.*, *Phys. Rev. B*, to be published.

[43] J.H. Brewer *et al.*, *Phys. Lett. A* **120**, 199 (1987).